Using Low-Altitude Meteorological Observations to Calculate the Mass Balance of Alaska's Columbia Glacier and Relate it to Calving and Speed

Wendell Tangborn
Seattle, Washington

Abstract

The 1949-96 mass balance of Columbia Glacier as a function of altitude and time is determined using low-altitude precipitation and temperature observations and the area-altitude distribution of the glacier (designated the PTAA model). In this report mass balance is defined as glacier surface changes only; losses from calving are considered separately. Algorithms are developed that convert precipitation and temperature observations to daily snow accumulation and ice and snow ablation for each 100 meter elevation increment of the glacier area. The thirteen coefficients that are used in these algorithms are solved simultaneously with a simplex optimization procedure. The PTAA model is calibrated by minimizing the error of fitting linear regressions between the simulated mass balance, snowline altitude, equilibrium line altitude and other balance variables; the model's underlying premise is that an internal consistency exists between these variables. The conformity of balance variables is determined by a unique relationship that exists between the regional climate and the area-altitude distribution of individual glaciers. A two-decade (or more) period of generally negative balances apparently triggered Columbia Glacier into drastic retreat, which now appears to be primarily controlled by seasonal runoff variations and water depth at the terminus. Glacier runoff, also simulated by the model, is applied to glacier speed and calving rate observations made during the retreat phase, from 1982-96, to demonstrate ice speed/intraglacial water storage and runoff/calving relationships.

Setting

The Columbia Glacier is located in Prince William Sound, Alaska. This large glacier (1030 square kilometers) is the last of the 51 tidewater glaciers in Alaska to make a drastic retreat. Disintegration of the lower glacier began in the late 1970s and full-scale retreat was underway in the early 1980s (Meier and others,1977; Meier and others, 1980). Since 1982 the terminus has retreated approximately 9 kilometers and the surface area of the glacier has decreased by 56 square kilometers, 12% of the ablation area.

The Prince William Sound climate at sea level is characterized by mild winters and cool summers. However, above 2500 meters, the temperature is seldom above freezing except for a few days in mid-July. Precipitation observed at sea level varies from 1700 mm annually (Seward) to 2400 mm (Cordova). There are no reliable precipitation records at higher altitudes in this region.

Model explanation

The mass balance at a specified altitude of a glacier is the difference between cumulative snowfall -- plus the redeposition of rain and meltwater by refreezing -- and cumulative ablation, summed from a reference date each year. January 1 was used as the reference date in this study to keep a distinct time separation between the annual and the net balance, measured at the time of minimum balance (which averages October 5, but varies from August 19 to November 12). The zero balance altitude (ZBA) is defined as the altitude that divides the positive and negative balance and is closely related to the glacier snowline altitude (SNL). The Equilibrium Line Altitude (ELA) is defined as the maximum altitude reached by ZBA each year. [ZBA could also be defined as a transient ELA.]

The time and space progression of the seasonal snowline is influential in determining the mass balance of a glacier. A rapidly rising snowline reflects a deficit winter snowpack and/or a high rate of summer snow ablation. A below-average snowpack also tends to produce greater total ablation because low albedo ice becomes exposed earlier in the season. A slowly rising snowline results from an above average winter snowpack and/or low snow ablation rates and tends to produce positive mass balances.

Snow accumulation (including the redeposition of refrozen rain and meltwater, which is found in this analysis to be measurable but inconsequential on Columbia Glacier), snow and ice ablation, and the resulting balance of the glacier (as a function of altitude and time) are calculated in this model from daily observations of precipitation and maximum and minimum temperatures recorded at nearby, sea-level weather stations (Seward, Valdez and Cordova) for the period 1949-96. These variables are determined each day for each area of the glacier differentiated by 100 meter elevation increments, from sea-level to 3300 meters. Thus there are 578,160 determinations each of ablation, accumulation, balance, runoff and other variables that are used in subsequent calculations.

The temperature for each elevation increment is found from the lapse rate, which varies according to the mean daily temperature anomaly and the daily temperature range. The lapse rate is critical in calculating both accumulation and ablation (a change of just 0.01 ^{O}C per 100 m can significantly alter the final balance results). There are four calibration coefficients used to calculate the lapse rate each day; two are the intercepts and two the slopes of the lines that relate lapse rate to the temperature range (Figure 1). Temperature inversions were not found to be significant.

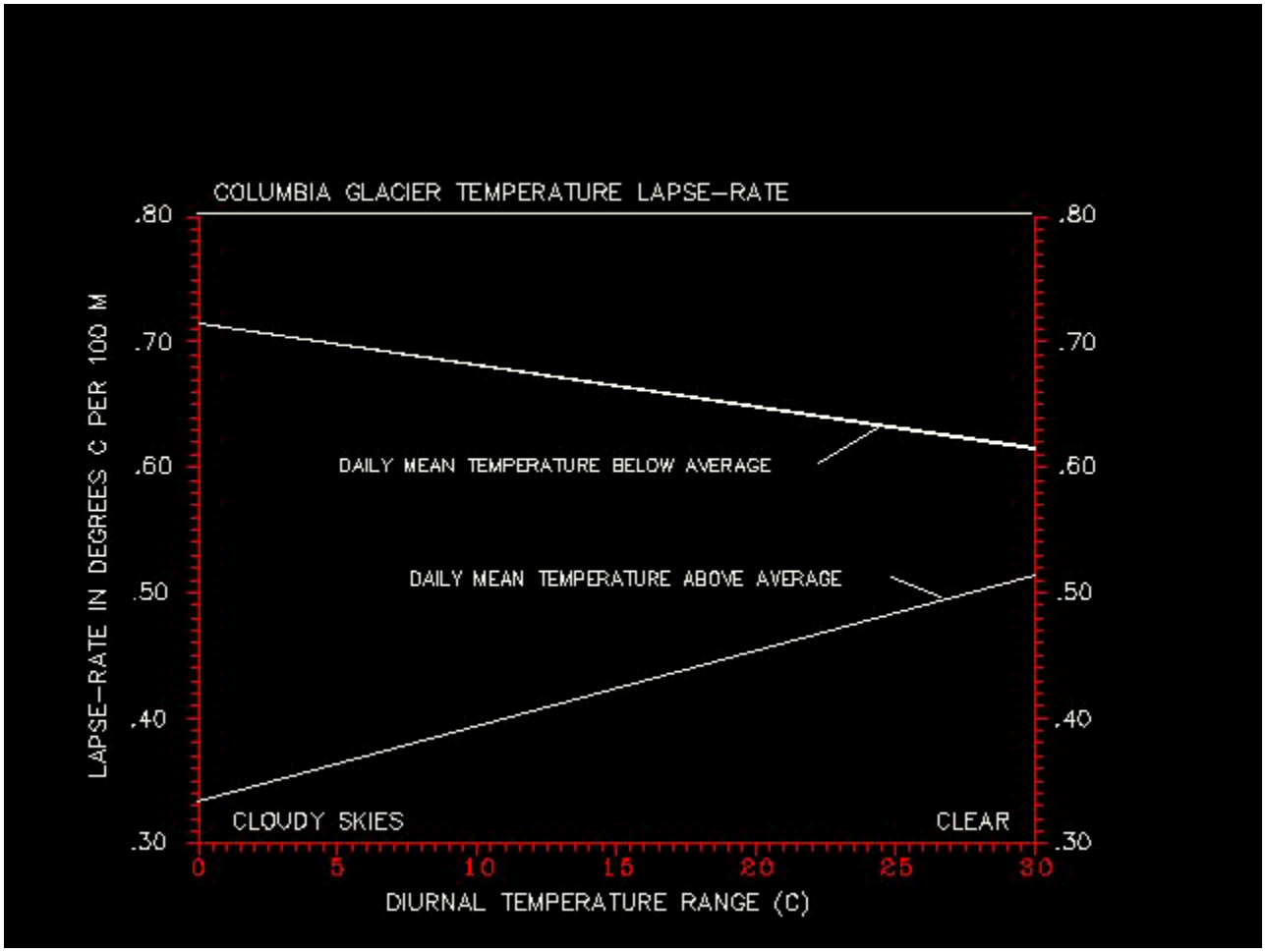

Figure 1. The temperature lapse rate is calculated daily from the temperature range (daily maximum minus minimum temperature) and the mean temperature anomaly (deviation of the mean daily temperature from the normal for that day) and from four calibration coefficients. Two coefficients are the intercepts of each line and two are the line slopes. These results generally agree with theoretical lapse rates. The saturated adiabatic lapse rate (i.e., on cloudy days) is less than the dry adiabatic lapse rate (lower line, above normal temperatures) and below normal temperatures (upper line), show a higher lapse rate on cool, cloudy days. The lapse rate declines as the temperature range increases (a high range on the upper line indicates skies are clear and the air is cold and dry).

The greater ablation rate of ice relative to snow is accounted for by a substantial decrease in the albedo below the snowline, which is controlled by one of the calibration coefficients. The glacier snowline altitude is lowered if a depressed freezing level occurs on days with precipitation, and is raised in accordance with the daily ablation rate above the snowline. The freezing level each day, as determined from temperature observations at sea level and the lapse rate, is therefore a significant factor for determining snow accumulation, ablation and mass balance. Ablation of snow and ice is calculated from

both the mean daily temperature and the temperature range, which provides a cloud-cover or solar radiation-melt index. Precipitation occurs as snow when the temperature is less than 0 ^{O}C at a specific altitude and as rain when it is above zero. Precipitation increases with elevation to a threshold level and is then constant to the highest elevation. The altitude distribution of mass balance is the difference between cumulative snow accumulation and cumulative ablation at each 100 meter altitude increment (Figure 2). The annual, winter and summer balances for the total glacier are found by applying the resulting balance/altitude distribution to the area-altitude profile. As the glacier retreats and loses area, it is necessary to adjust the AA profile continuously.

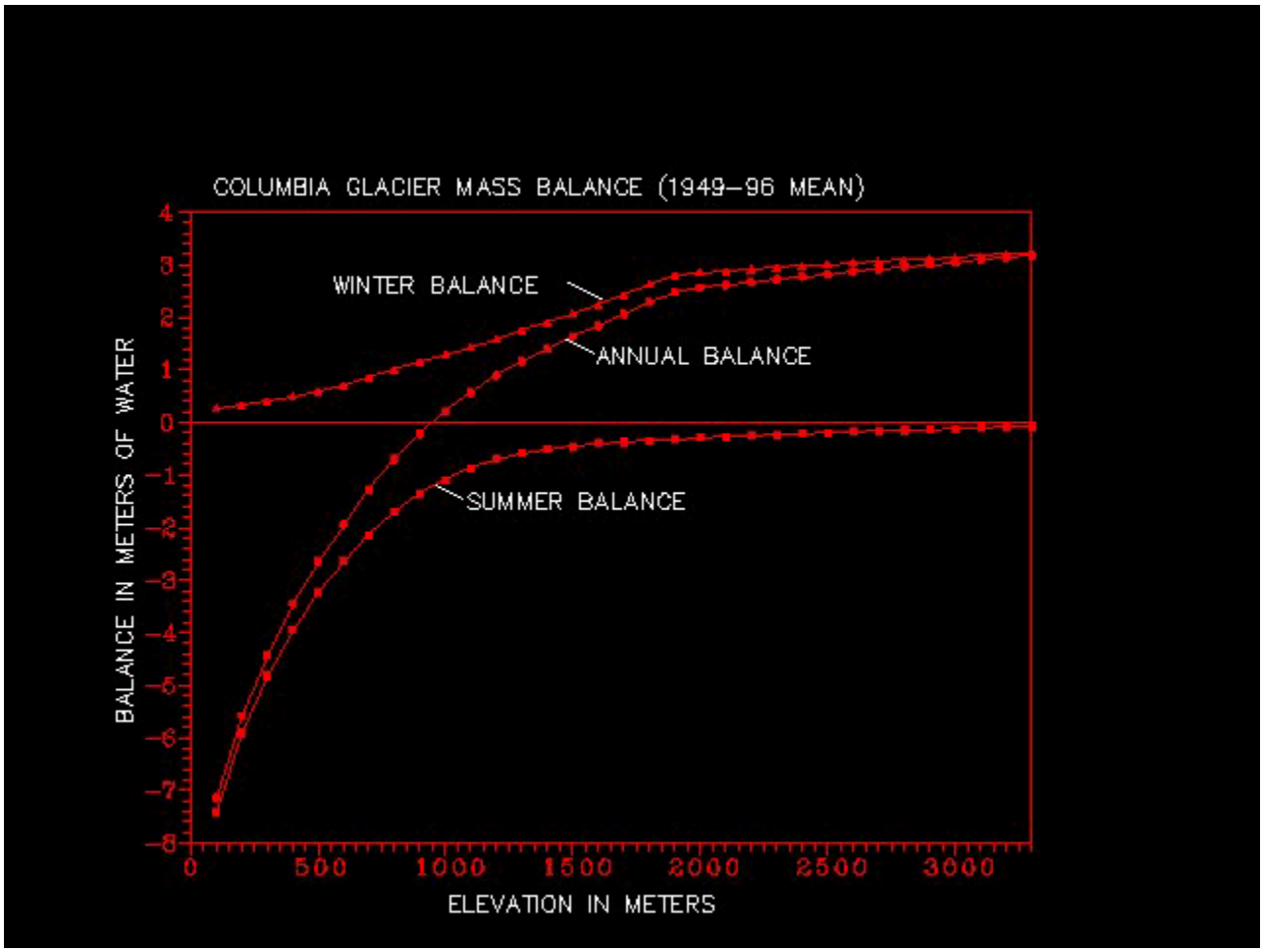

Figure 2. The mean annual, winter and summer (surface) balances averaged for the 1949-96 period, calculated for each 100 meter altitude increment. The average winter balance for this period is 1.72 m(we), the average summer balance, 1.33 m(we), and the annual balance, +0.39 m(we).

The cumulative mass balance for the 1949-96 period is shown in Figure 3, and the annual, winter and summer balances for each year in Figure 4. There was an abrupt change in mass balance about 1970, apparently due to both an increase in snow accumulation (winter balance) and a decrease in ablation (summer balance). There is a

positive feedback mechanism linking winter and summer balances because an increase in snow accumulation lowers the ELA producing a significant decrease in ice ablation.

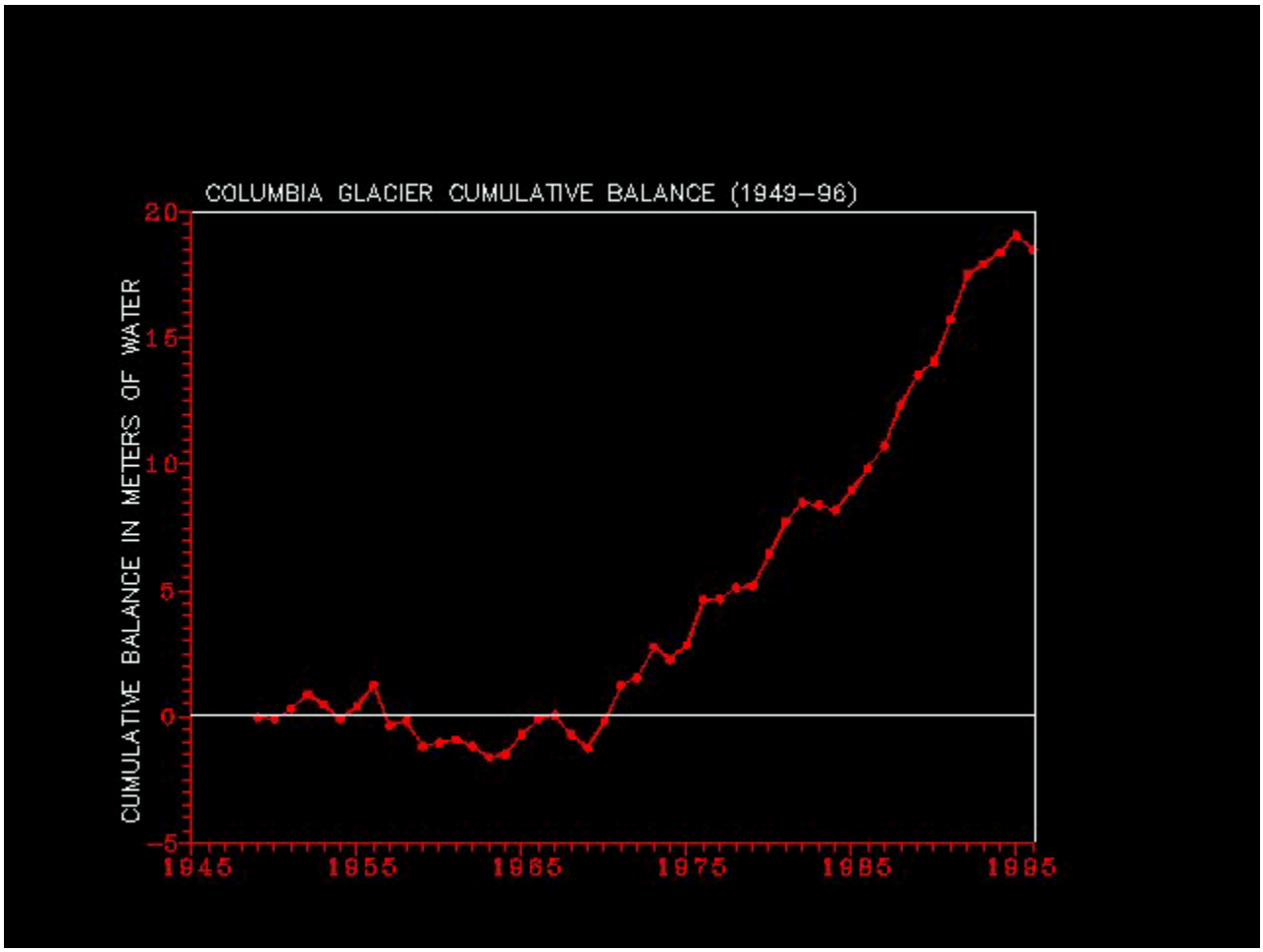

Figure 3. Neglecting calving losses, the cumulative annual balance for the period of record indicates a period of generally negative balances from 1949 to about 1974, then mostly positive balances since then. After 1982, when a pronounced retreat began and the ablation area is reduced in size each year, there would be a tendency for the balances to be more positive because of less ice melt. However, this is not thought to be the main cause for the recent 20-year period of positive balances. See Figure 7 for balance results that include calving losses.

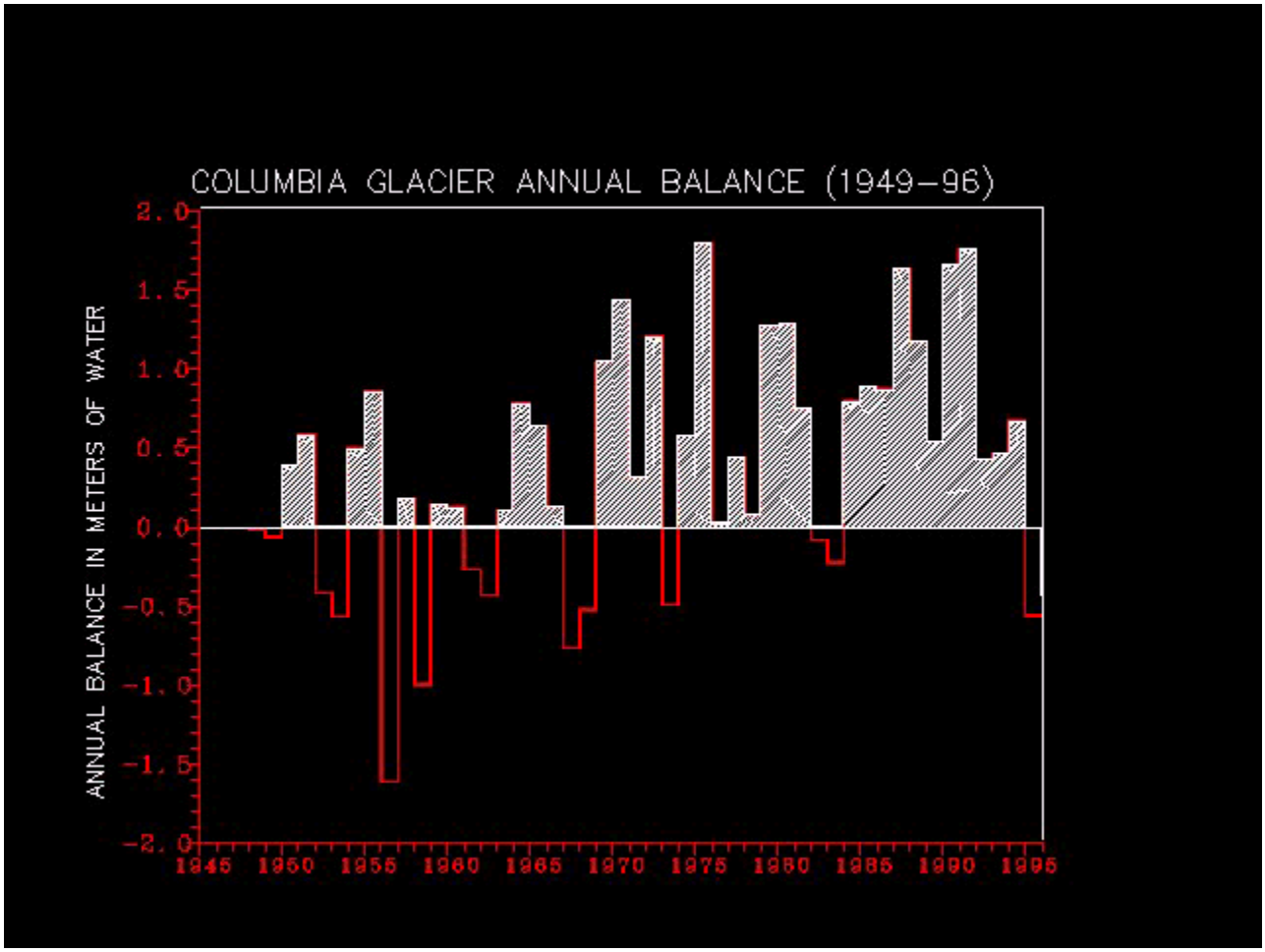
COLUMBIA GLACIER ANNUAL BALANCE (1949–96)
ANNUAL BALANCE IN METERS OF WATER
2.0
1.5
1.0
0.5
0.0
-0.5
-1.0
-1.5
-2.0
1945
1950
1955
1960
1965
1970
1975
1980
1985
1990
1995

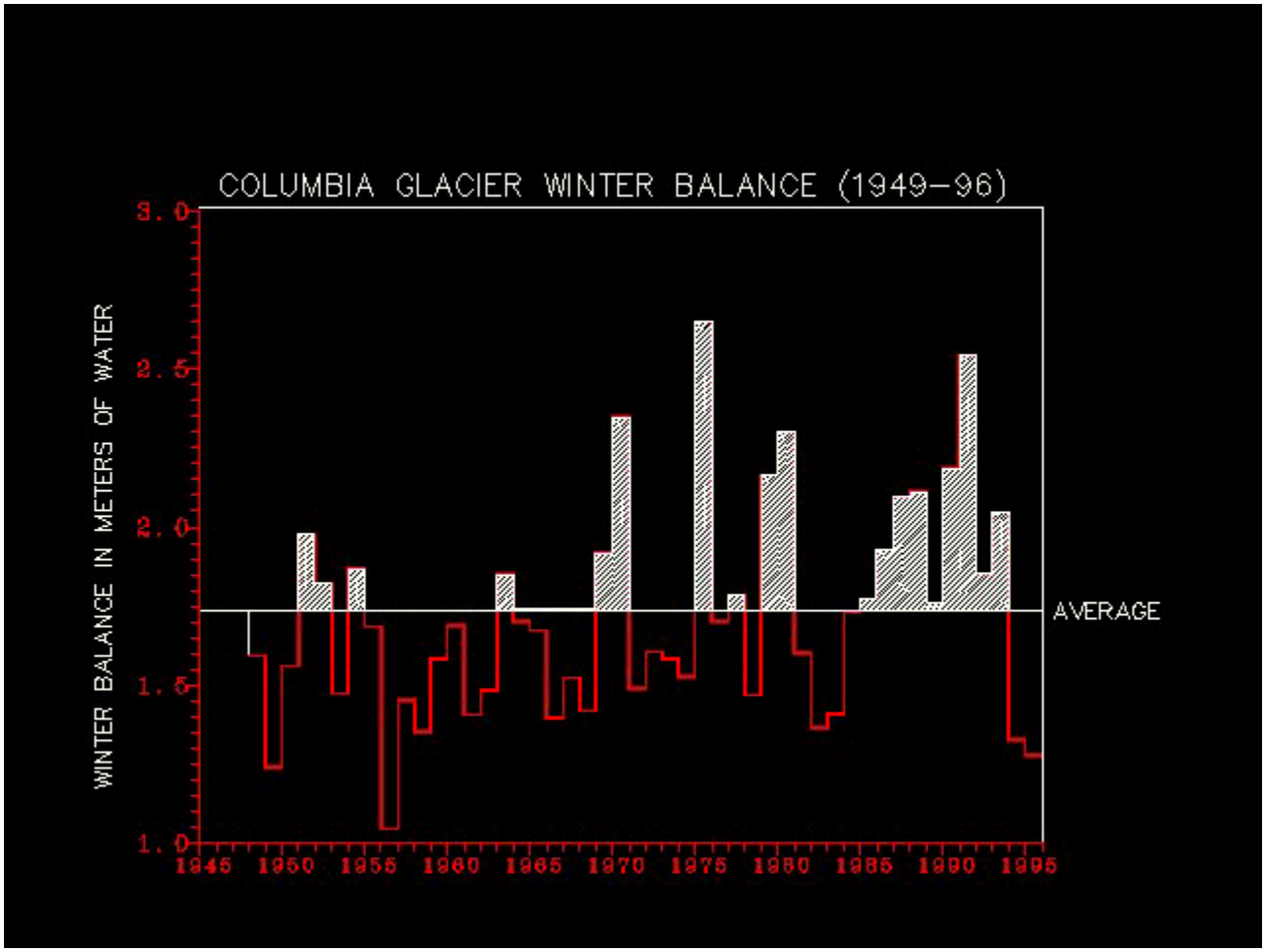
COLUMBIA GLACIER WINTER BALANCE (1949–96)
WINTER BALANCE IN METERS OF WATER
3.0
2.5
2.0
1.5
1.0
AVERAGE
1945
1950
1955
1960
1965
1970
1975
1980
1985
1990
1995

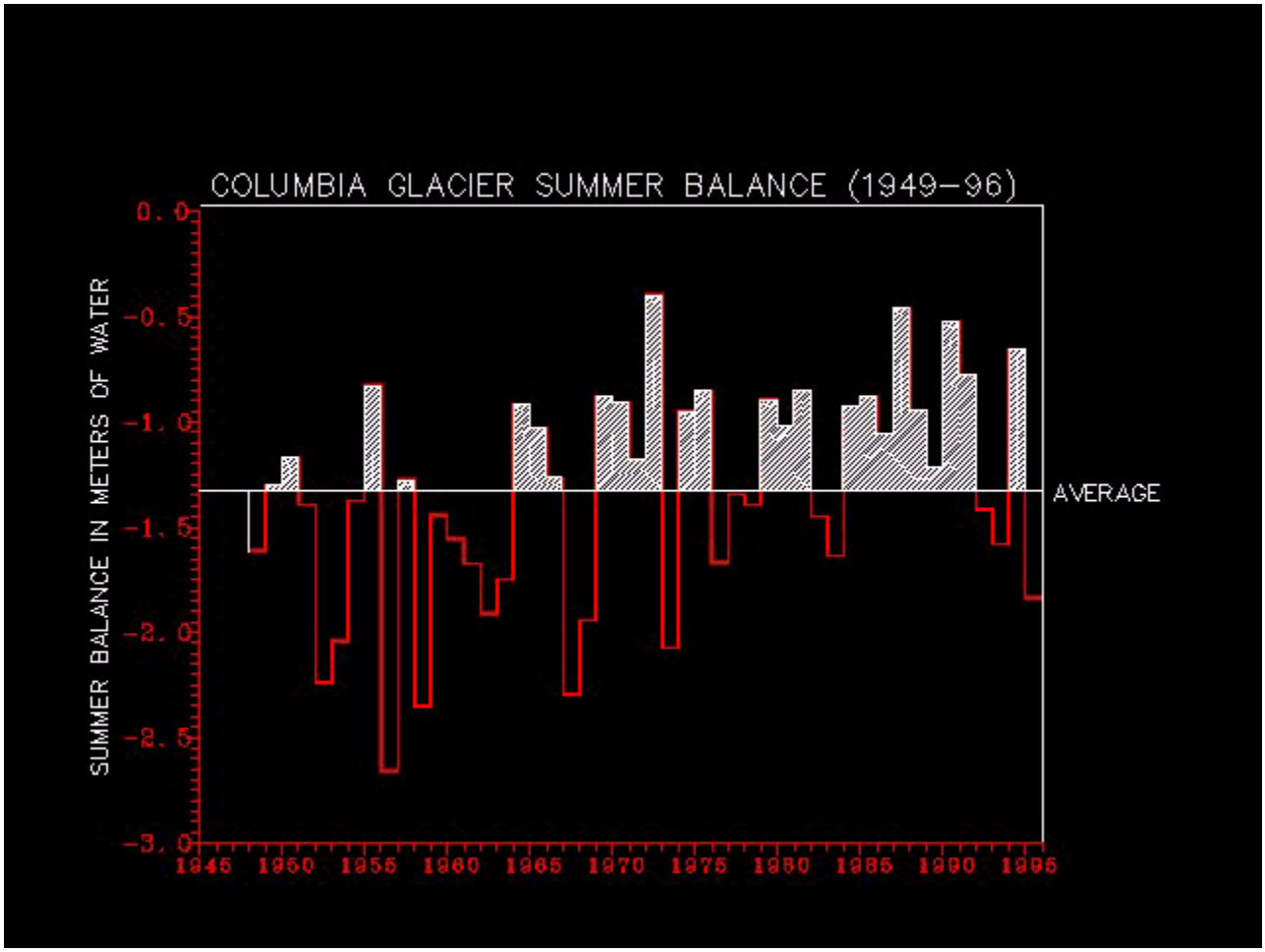

Figure 4. Annual balances (top panel), winter balances (middle panel) and summer balances (lower panel) from 1949 to 1996, measured each year from January 1 to December 31.

The area-altitude profile of a glacier evolves from the erosional effects of ice movement during the thousands (or even millions) of years of its existence, and it is the space and time distribution of the mass balance that controls ice discharge and erosion rates. As the mass balance is determined by the climate, the current AA profile of Columbia Glacier is then thought to have memorized climate conditions during the thousands of years of erosion and the ensuing isostatic uplift (Pinter and Brandon, 1997; Brozovic and others, 1997). Therefore, embedded in the present day area-altitude distribution is the key to relating climate and mass balance. A climatic trace likely remains in the AA profiles of all glaciers. It may be nearly obscured by the geometry induced by regional geology for some glaciers; however, some climatic remnant of past eons probably exists in most of them. The underlying premise of the PTAA model is that an internal consistency exists between the distribution of the mass balance and the altitude of the snowline and equilibrium line. The connection between them controls the glacier's area-altitude profile (Tangborn and others, 1990).

Model calibration

The model is calibrated by simultaneously estimating the value of 13 coefficients in algorithms that convert daily precipitation and temperature observations to snow accumulation and snow and ice ablation. Several of these algorithms were developed and used in an earlier study (Tangborn, 1980). Coefficient optimization is accomplished by a simplex minimization procedure that uses as an objective function the error of a linear fit between several of the variables that are calculated annually (Nelder and Mead, 1965); most of these relationships are dependent on the area-altitude distribution. For example, a linear fit between the snowline altitude and zero balance altitude (SNL and ZBA); or between annual mass balance and the ELA; and between the energy of glacierization (Shumskiy, 1946) and the ELA, are all used for coefficient optimization. There have been several previous studies relating mass balance and the energy of glacierization to the ELA (LaChapelle, 1962; Braithwaite, 1984).

The period used for calibration was 1949-82 to avoid the inaccuracies caused by continuous area changes of the lower glacier as it retreated during the 1983-96 period. For the full period (1949-96), a revised area-altitude distribution is estimated for each year to calculate the annual mass balance and other variables.

Model verification

Independent verification of the PTAA model's mass balance results is not possible on an annual basis; however, there was one large-scale effort made to measure the mass balance in 1977-78 by the U.S. Geological Survey (Mayo and Trabant, 1978; Mayo and others, 1983). A comparison of the measured 1977-78 balance with that calculated with the PTAA model is shown in Figure 5. Except for the two highest elevation points, there is a good agreement between the measured and modeled balances for that year.

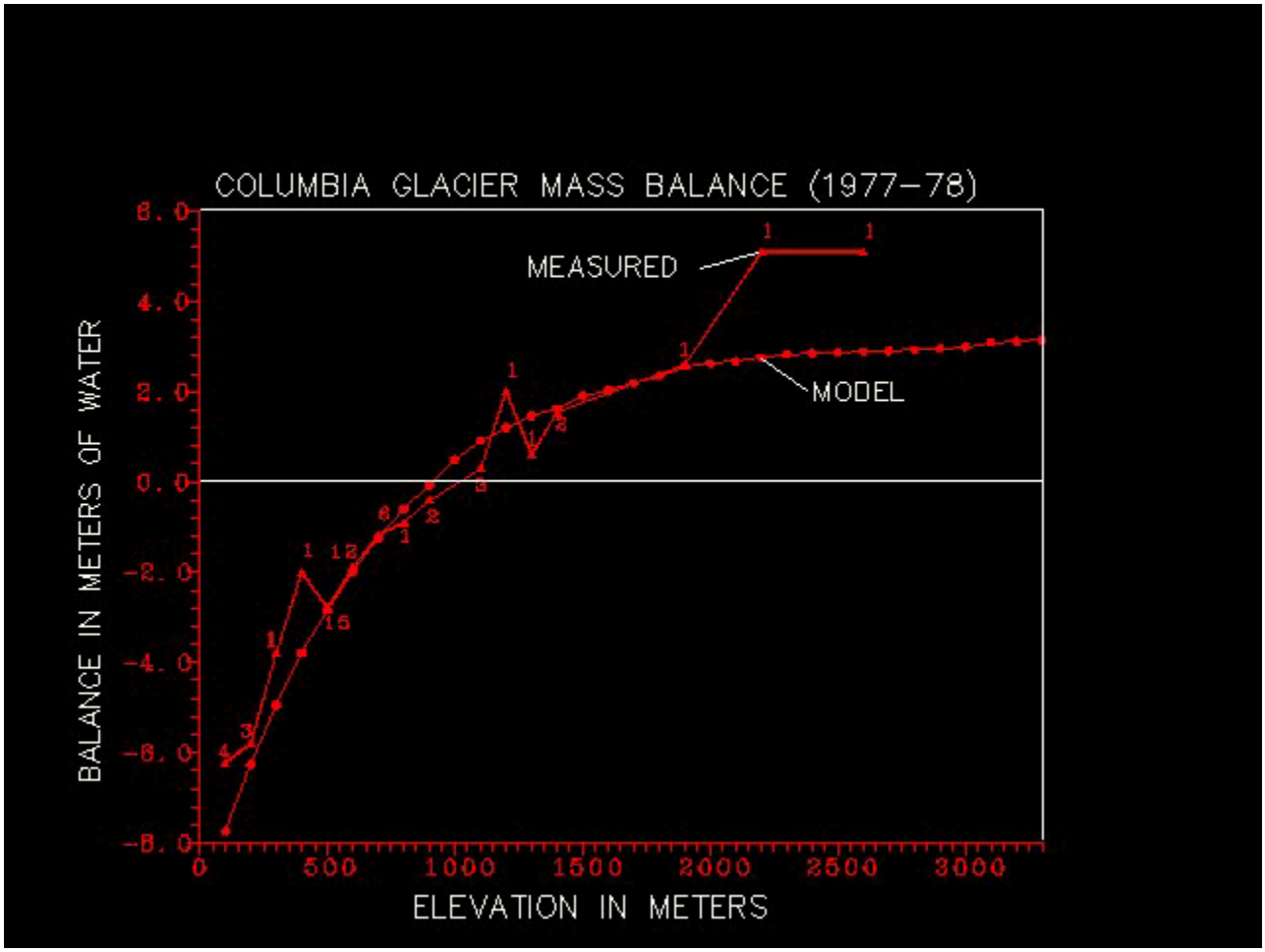

Figure 5. A comparison between measured (Mayo and others, 1979) and modeled mass balance results for the 1977-78 balance year. Triangles are the average measured balance within 100 meter elevation intervals, based on observations at ablation/accumulation stakes (numbers refer to stakes read within each interval). Model balances are averaged for each 100 meter interval (circles) and are based on a 1949-82 calibration period. The measured annual balance for 1978 is +790 mm; the modeled balance is +444 mm.

Another attempt to measure the mass balance at specific points above the ELA was made in 1996 (Austin Post, pers. comm.), by measuring the depth of snow accumulation to an ash layer deposited in September of 1992 by an eruption of Mt. Spurr (Figure 6). These measurements, made at 1130, 1340 and 1740 meters, also show fair agreement with the model's average 1993-96 balance at these altitudes. Additional field measurements of balance above 1500 m are needed to verify the model's balance results.

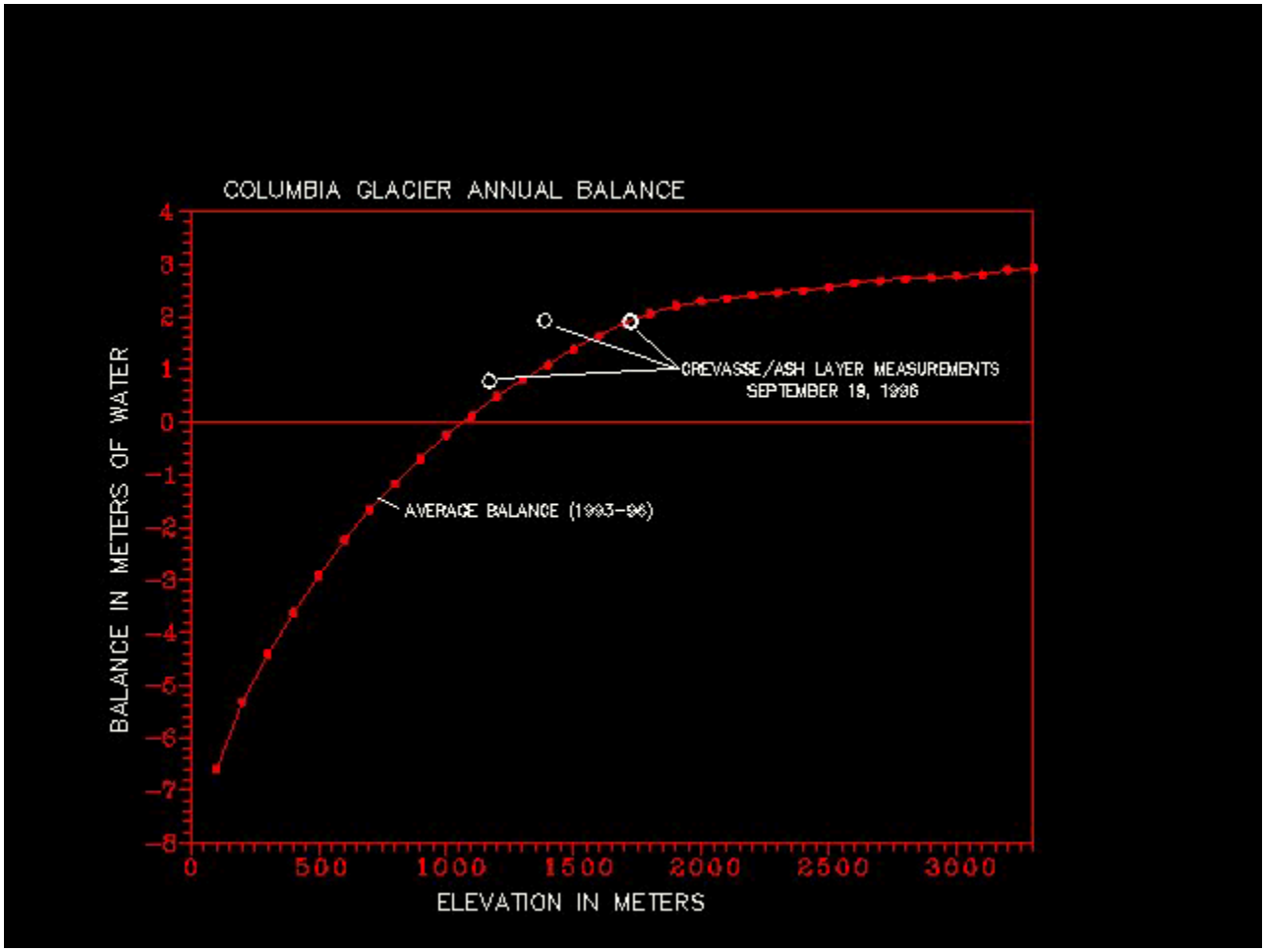

Figure 6. The eruption of Mt. Spurr (300 km to the NW) in September 1992 deposited a heavy ash layer over most of Columbia Glacier. Austin Post measured the depth below the snow surface of this ash layer at three points four years later, on September 19, 1996, by having the helicopter descend into large crevasses and using the altimeter to determine snow depths. The three measurements, at approximately 1740 m, 1340 m and 1130 m, showed snow depths of 15 m at the two higher sites and 6 m at the lower site. Assuming a mean density of 0.50, the average annual balance since the eruption would then be 1.90 m(we) at the high elevation sites and 0.8 m(we) at the lowest site. The average balance determined by the PTAA model is shown for the four year period (1993-96) since the eruption.

Another means of verification is demonstrated by the long-term volume change of Columbia Glacier, determined from both surface balance changes and calving losses (Figure 7). Annual calving losses were estimated from 1949 to 1981 based on calculations of terminus area and velocity for one year, 1978 (Brown and others, 1983), and by assuming the annual loss during the relatively stable pre-retreat period was constant. Calving rates since 1981 are based on measurements of velocity and terminus positions derived from aerial photography, plus below sea level losses determined by bathymetry of the forebay between the terminus and terminal moraine shoal (Krimmel,

pers. comm.). An independent volume change for the 1957-1994 period has been determined from a airborne Laser/GPS system (Echelmeyer, pers. comm.) and is also shown in Figure 7.

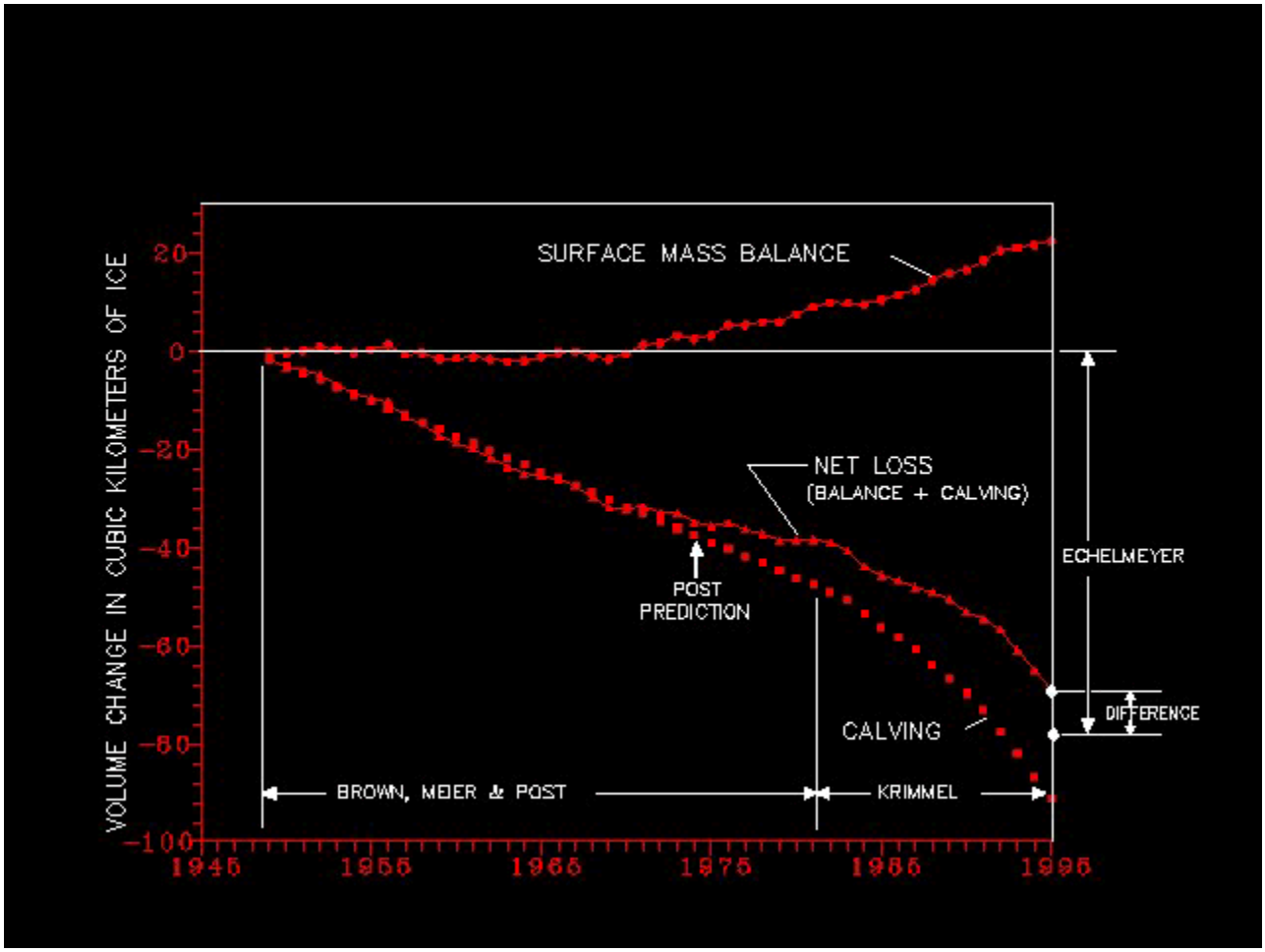

Figure 7. Preliminary results of glacier's volume change since 1949, based on mass balance, calving and elevation changes. Calving rate from 1949-1981 is derived from pre-retreat calculation of calving speed and terminus surface area (Brown and others, 1982). Since 1981, calving rate is based on velocity at terminus and retreat rate, calculated by Krimmel from aerial photographs taken about 5 times per year. Total volume loss estimated by Echelmeyer from elevation changes mapped between 1957 and 1994 and the area-altitude profile of the glacier (-70 km3) plus below sea level loss from forebay (-7.5 km3).

Verification of model results can also be done by comparing simulated runoff with measured runoff at a nearby glacier. Average annual runoff of the glacierized Knik River basin, which was gauged by the U.S. Geological Survey from 1960-1987, is 2.02 m. Simulated runoff of Columbia Glacier for the same period is 2.45 m. The difference is not thought to be significant because of several other variables (see following section).

Glacier runoff

One by-product of modeling the mass balance is glacier runoff, which is defined as the sum of total ablation (ice and snow) plus precipitation that occurred as rain (Figure 8). The measured runoff of the Knik River, which is from a 54% glacierized watershed approximately 90 kilometers northwest of Columbia Glacier, is shown as an independent comparison of Columbia Glacier runoff. The total runoff volumes from the Knik and Columbia Glaciers are similar, but peak runoff of the Knik River occurs about two months earlier, for several possible reasons: 1) because of geographic-induced differences in precipitation and ablation rates, 2) the Knik River runoff observations include non-glacierized areas and 3) intraglacial storage is accounted for in the Knik River record but not in Columbia Glacier's simulation.

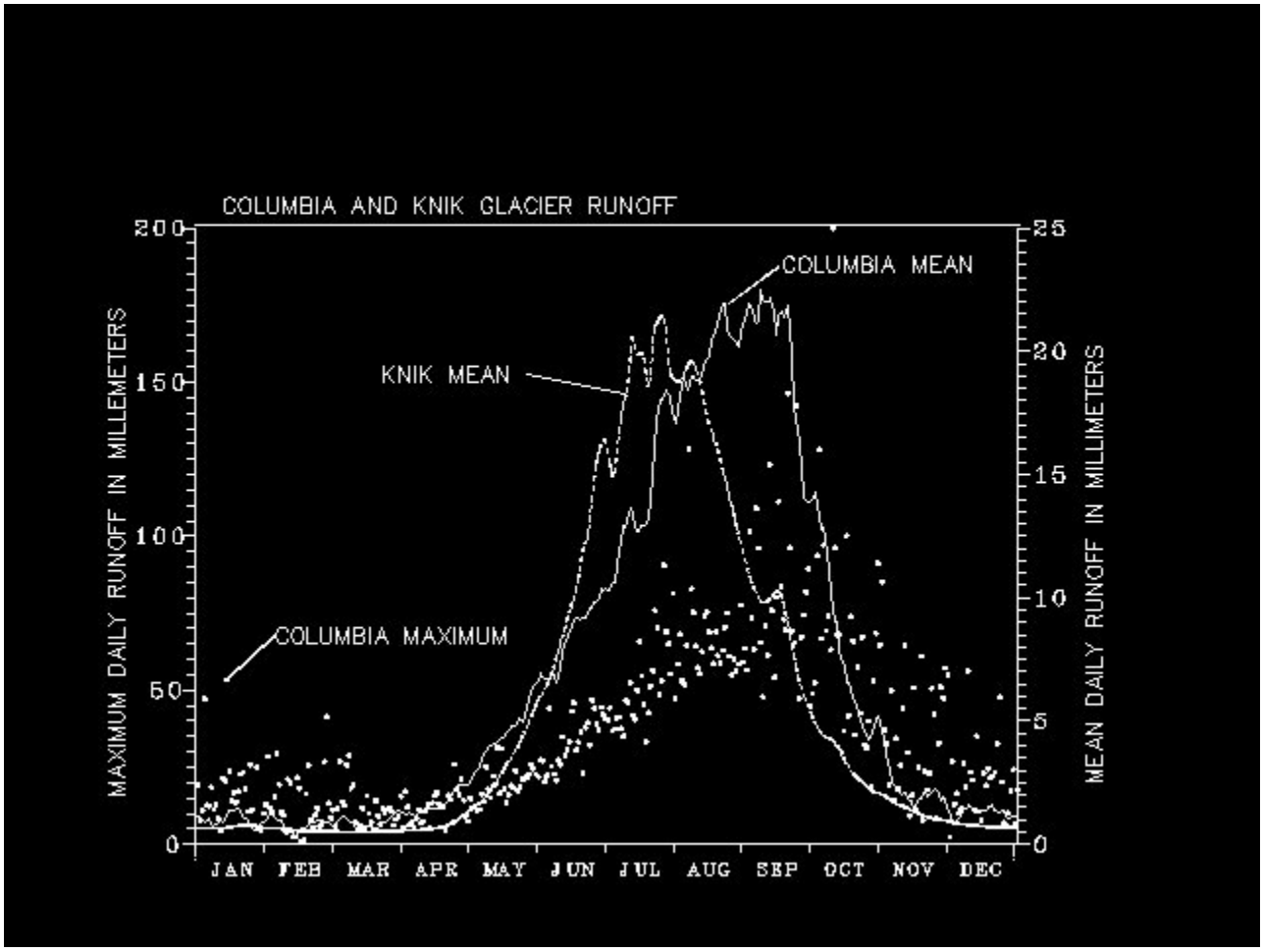

Figure 8. Runoff from Columbia Glacier is generated each day by the PTAA mass balance model and is the sum of precipitation occurring as rain plus ablation of ice and snow, both averaged over the total area of the glacier. The mean daily runoff is a solid line; maximum runoff that has occurred each day of the year during the 1978-94 period is shown as dots. The measured mean daily runoff of the Knik River, which is 54% glacierized, is shown for comparison (dotted line).

Runoff is generated daily in the model at each 100 m altitude interval, then summed for each area increment over the entire glacier. Water originating at the glacier surface moves rapidly through the ice, enlarging passageways as it travels, and some runoff eventually reaches the glacier bed. Basal water pressure of Columbia Glacier has been shown in a 1987 study to be directly related to glacier movement by basal sliding (Meier and others, 1994; Kamb and others, 1994). In the 1987 study, diurnal fluctuations in basal water pressure are measured along with fluctuations in sliding speed.

There are indications that changes in the influx of water into the glacier near the terminus control calving rates. The significant seasonal variations in both velocity and calving rates, which are nearly 180 degrees out of phase, are likely controlled by seasonal changes in runoff. Unusually high discharge events (an order of magnitude greater than normal runoff) may be the primary cause of the massive release of icebergs at the glacier terminus.

There is observational evidence that Columbia Glacier velocity is greatest in the spring (mid-March) and that the calving rate is greatest in the autumn (mid-September) (Krimmel, this volume).

There is other evidence of a dynamic relationship between calving rate and maximum runoff events throughout the year, as demonstrated in Figure 9 and suggested in an earlier study (Sikonia and Post, 1980). The calving rate (shown as a solid line in Figure 9) is calculated from velocity and recession measurements based on 66 aerial photography flights during this 17-year period (Krimmel, pers. comm.). Daily calving rates were estimated by a straight-line interpolation for the intervals between the photographic overflights, which average 94 days in length. The resulting "saw-tooth" record was then averaged for each day for the 1978-94 period. The maximum daily runoff that occurred during the 17-year period (shown as dots in Figure 9) is the sum of total ablation and rain over the entire glacier. These maximum discharge events appear to be related to high calving rates more than daily mean runoff.

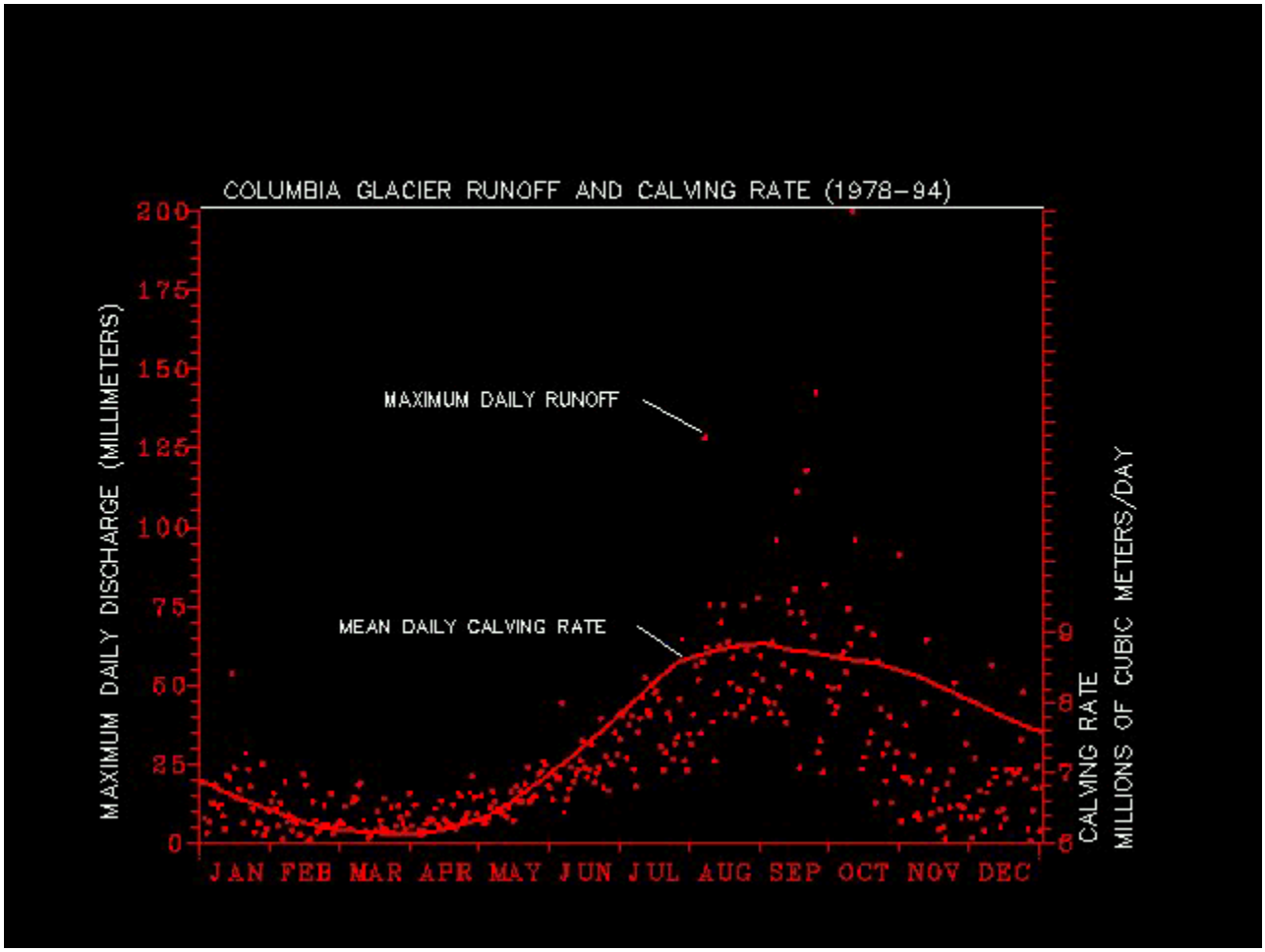

Figure 9. The average calving rate (solid line) is based on 66 measurements of glacier speed and terminus positions calculated from aerial photographs, taken at an average time interval of 94 days (Krimmel, this volume). Maximum runoff rather than the daily average is shown because the highest runoff events appear to have the greatest influence on calving.

It has been suggested that the basal storage of water during the autumn and winter accounts for the maximum ice velocities observed on Columbia Glacier in the spring (Van der Veen, 1995). Intraglacial water storage can be derived from simulated runoff by assuming that if daily discharge is less than a specified threshold, it is stored within the glacier; if it is greater than the threshold there is instead a release from storage. The rationale for this simple model is that a large input of water tends to open drainage conduits, and when runoff is low the conduits are closed by glacier movement. Intraglacial water storage is calculated from daily simulated runoff by:

$$XR(i) = R(i) \text{ when } R(i) < R_x ,$$

$$S(i) = \Sigma\, XR(i) ,$$

and

$$Q(i) = C_x S(i) \text{ when } R(i) > R_x ,$$

then

$$S(i) = S(i-1) + XR(i) - Q(i) ,$$

where

$XR(i)$ = Runoff that is less than the threshold on day i,

$S(i)$ = Water storage averaged over the glacier area on day i,

$R(i)$ = Simulated runoff averaged over glacier area on day i,

$Q(i)$ = Discharge of water from storage on day i (mm),

R_x = Runoff threshold (mm),

C_x = Storage release coefficient.

The storage summation is continuous from January 1, 1949 to December 31, 1996. The release of water from storage is assumed to be directly dependent on the amount of water that is in storage (the hydrostatic head), and independent of runoff volumes; once the drainage channels have enlarged, the magnitude of surface runoff is assumed to be inconsequential in releasing water from storage. Average water storage calculated by this model throughout the year, averaged for the total glacier area, is demonstrated in Figure 10. As 90% of runoff produced is below the ELA, actual storage amplitude over the lower glacier would likely be more than two times that shown. The timing and magnitude of intraglacial water storage shown for Columbia Glacier is similar to that found for South Cascade Glacier, Washington (Tangborn and others, 1975).

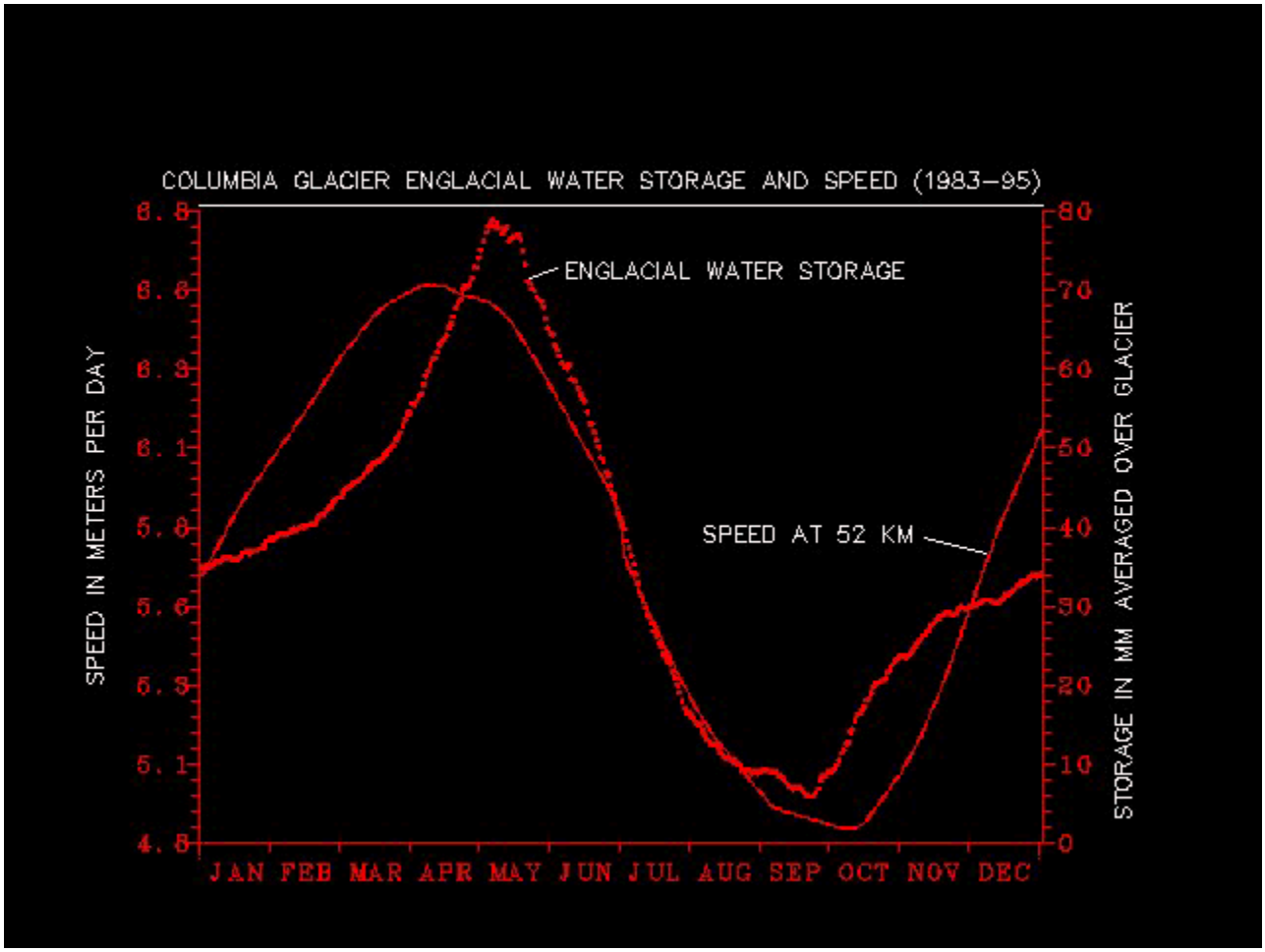

Figure 10. Intraglacial water storage is derived from simulated runoff (precipitation as rain plus ablation). The assumption is made that if daily runoff is less than a specified threshold it is stored within the glacier. If runoff exceeds the threshold there is a release of water from storage; the rate of release is dependent only on the amount of storage. The rationale for this model is that a large input of surface water tends to open drainage conduits. When runoff is low, the conduits are closed by glacier movement. Glacier speed is measured from crevasse position changes plotted from a 15-year sequence of 66 aerial photographs, then averaged for each day over the period of record.

To produce these results, a threshold value of 6 mm (slightly less than mean daily runoff) was used for R_x, and a value of 0.10 for C_x. Using these coefficients, maximum storage for the total glacier occurs on an average date of approximately May 5; for individual years, the time of maximum storage varied from March 20 to July 3 (varying these coefficients does not substantially affect the time of maximum storage but does alter the amplitude).

Relationship of ice speed and calving to runoff

Based on the evident connection between ice speed and intraglacial water storage shown in Figure 10, and between calving rate and high runoff events shown in Figure 9, there is compelling empirical evidence that both sliding speed and calving are hydrologically controlled. The relationships shown between the above variables likely are different for the pre-retreat period and since retreat began, therefore each would require a separate analysis. A major portion of the ice speed and calving data has been collected during the retreat phase, so a detailed analysis before retreat began is not possible.

Columbia Glacier's first major retreat in 2000 years may be at least partially due to a critical amount of thinning associated with two decades (1950-70 or more) of negative balances (see Figures 3 and 4 (top panel)). However, there is an inexplicable decade between the end the period of generally negative balances to the beginning of the retreat. Even though the mass balances from about 1974 to 1982 were mostly positive, apparently the mechanism controlling massive ice loss at the terminus had already been set in motion before this, and retreat was inevitable.

As early as 1974, Austin Post suggested imminent retreat based on the formation of deep embayments at the terminus (Post, 1974); he repeated this prediction in subsequent years (Post, 1977). By 1979 the glacier had separated from Heather Island and has remained separated since then for the first time since observations began (Van der Veen, 1996). Once retreat began, the glacier's mass balance, even though predominately positive, was probably inconsequential in influencing retreat rate.

Prior to about 1980, while the glacier was jammed against the moraine, there was probably less fracturing in the area above the terminus than there is now. Because there were fewer deep vertical channels in the ice, less surface water reached the bed and runoff may not have played such a significant role in ice speed and calving before retreat began. Once the glacier was free of the confining moraine, large horizontal stresses would have developed within this 200-300 meter high ice front and extended up-glacier for at least this distance. Large, deep crevasses would be more common, allowing surface water to penetrate deeper into the glacier. Increased sliding speed in the area near the terminus would then be expected, and is found, due to greater water pressure at the bed.

A 500% increase in both lower-glacier speed and calving rate has occurred since retreat began (Meier, 1994; Krimmel, 1996). The causes of these spectacular increases are not fully known; however, it can be reasoned that the increased calving rate is partially caused by the increase in ice speed. Explaining the cause of the recent acceleration in ice motion would then at least partly explain the greater calving rates that have occurred since the early 1980s. Calving rate is diminished in the winter and spring when the surface water supply is shut off, but this is when water storage and basal sliding increase. Rapid retreat has been occurring from about 1982 to the present because the calving rate is greater than ice replenishment, which is dependent on glacier speed.

Observations on the Unteraargletscher in Switzerland suggest that water pressure at the bed, rather than total water volume, is the controlling factor for sliding speed, which increases when bed roughness is reduced by uplift (Iken and Bindschadler, 1986).

Maximum ice speed was also found in the spring in this case, when runoff rates were the highest. It could be argued that bed water pressure is likely to be directly proportional to volume so that velocity should show a direct dependency on water storage.

There has been an apparent increase in maximum water storage within the glacier each year during the past half-century (Figure 11). The cause of this increase is unknown but is likely related to a subtle change in runoff patterns, which is more a reflection of a change in meteorological variables than a physical change within the glacier. One possible connection is that the loss of ablation area reduces high rates of ice ablation, which increases the tendency of runoff to go into storage. The increase of maximum water storage with time may be partially responsible for the increase in sliding speed, but it is likely a minor component.

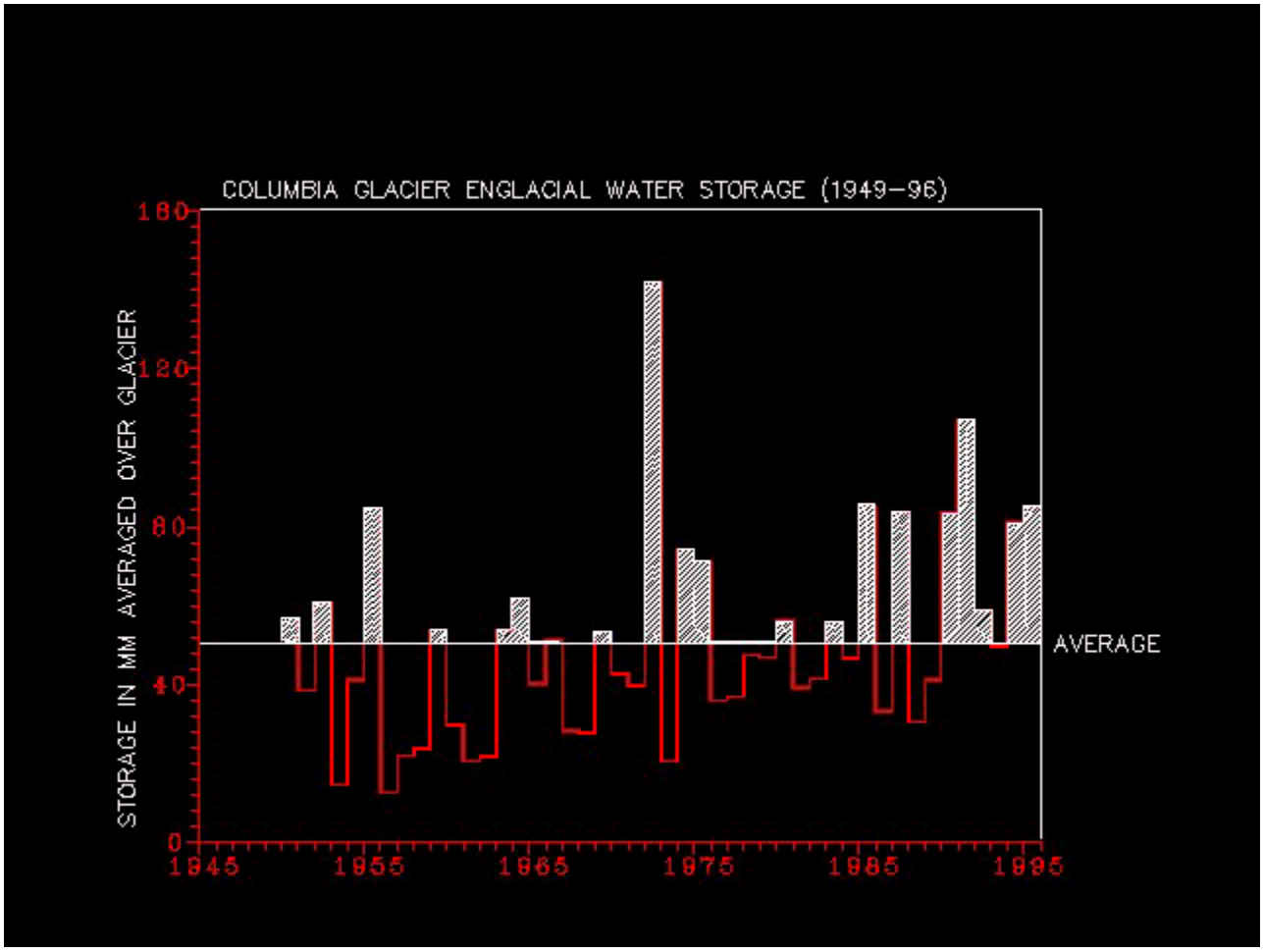

Figure 11. Maximum intraglacial storage each year for the 1949-96 period appears to be increasing. The reason is not an increase in runoff, but more likely a decrease in runoff intensity due to a reduced ablation area.

The increase in ice speed is by far the greatest on the lower part of the glacier, below about 50 km, suggesting that since about 1982 the hydrologic connection from the

surface to the bed is the most established in this region. The fact that the seasonal timing of ice (sliding) speed and calving rate are 180 degrees out of phase, and that both display similar power law relationships to runoff, seems significant. However, the runoff variable that appears to influence calving (daily maximum) is inversely correlated with the intraglacial storage of water, because high discharge events tend to open drainage channels within the glacier, thus releasing water from storage.

The role of mechanical energy derived from flowing water would tend to open and enlarge passageways and weaken ice bonds (Hooke, 1984). An increase in the break-off of ice from the terminus would then occur as the amount of runoff increases, likely aided by the buoyancy effect of seawater penetrating into the fractured zone, and by stresses produced by ocean tides, which have a diurnal range as high as 5 meters in Columbia Bay (Walters, 1989).

A cause-and-effect mechanism relating runoff with both speed and calving increases is suggested by a plot of monthly means of water storage versus monthly means of glacier speeds (Figure 12) and monthly means of maximum daily runoff versus mean calving rates (Figure 13). It may be noteworthy that in both of these relationships the best fit of the data suggests similar power laws of the form: y = axn.

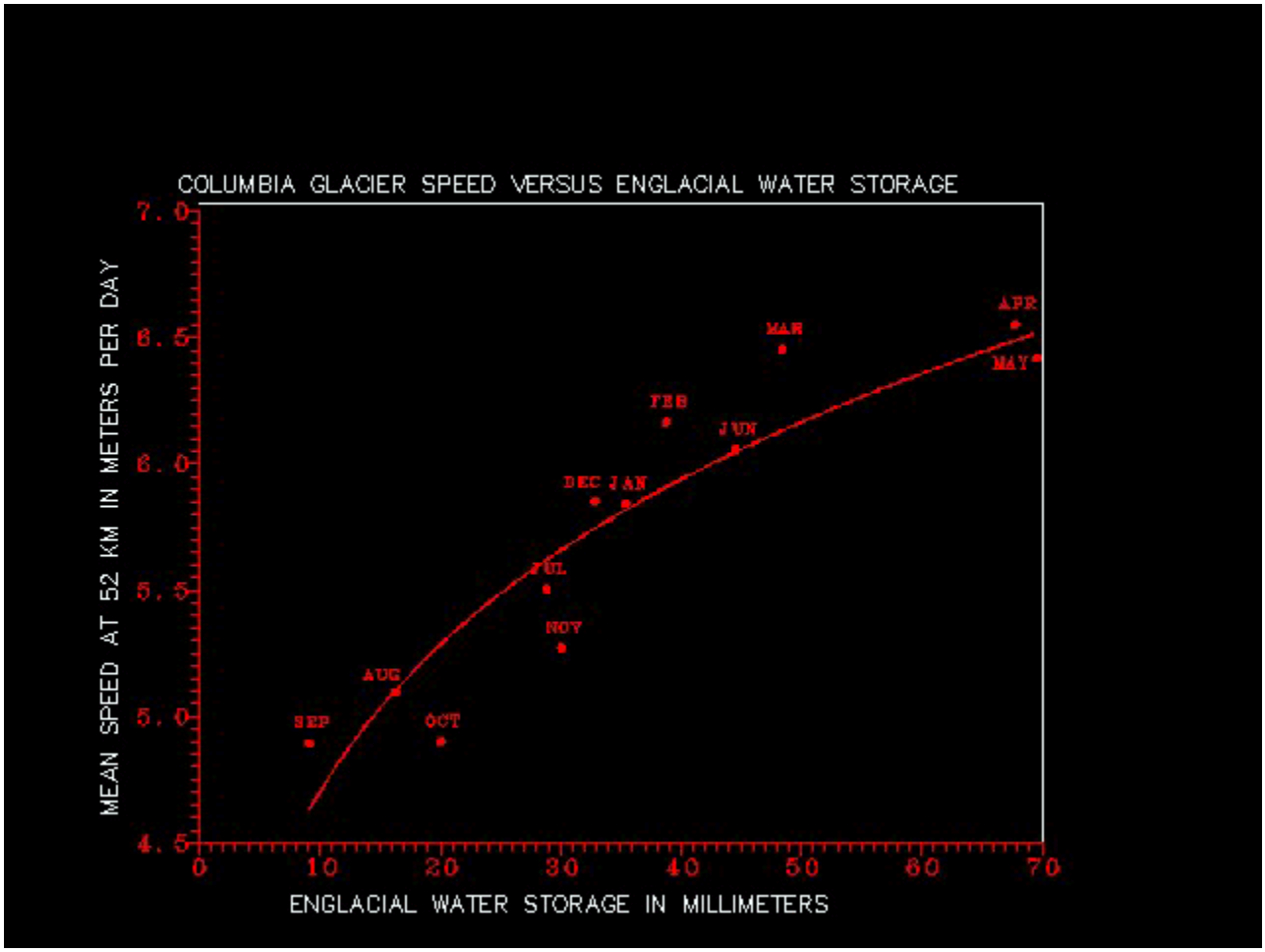

Figure 12. The average monthly storage of intraglacial water derived from simulated runoff is related to monthly averages of observed glacier speed at the 52 km distance down glacier, for the 1983-95 period. Note that there is a close similarity of the relationship between water storage and glacier speed, to maximum runoff and calving rate shown in Figure 13.

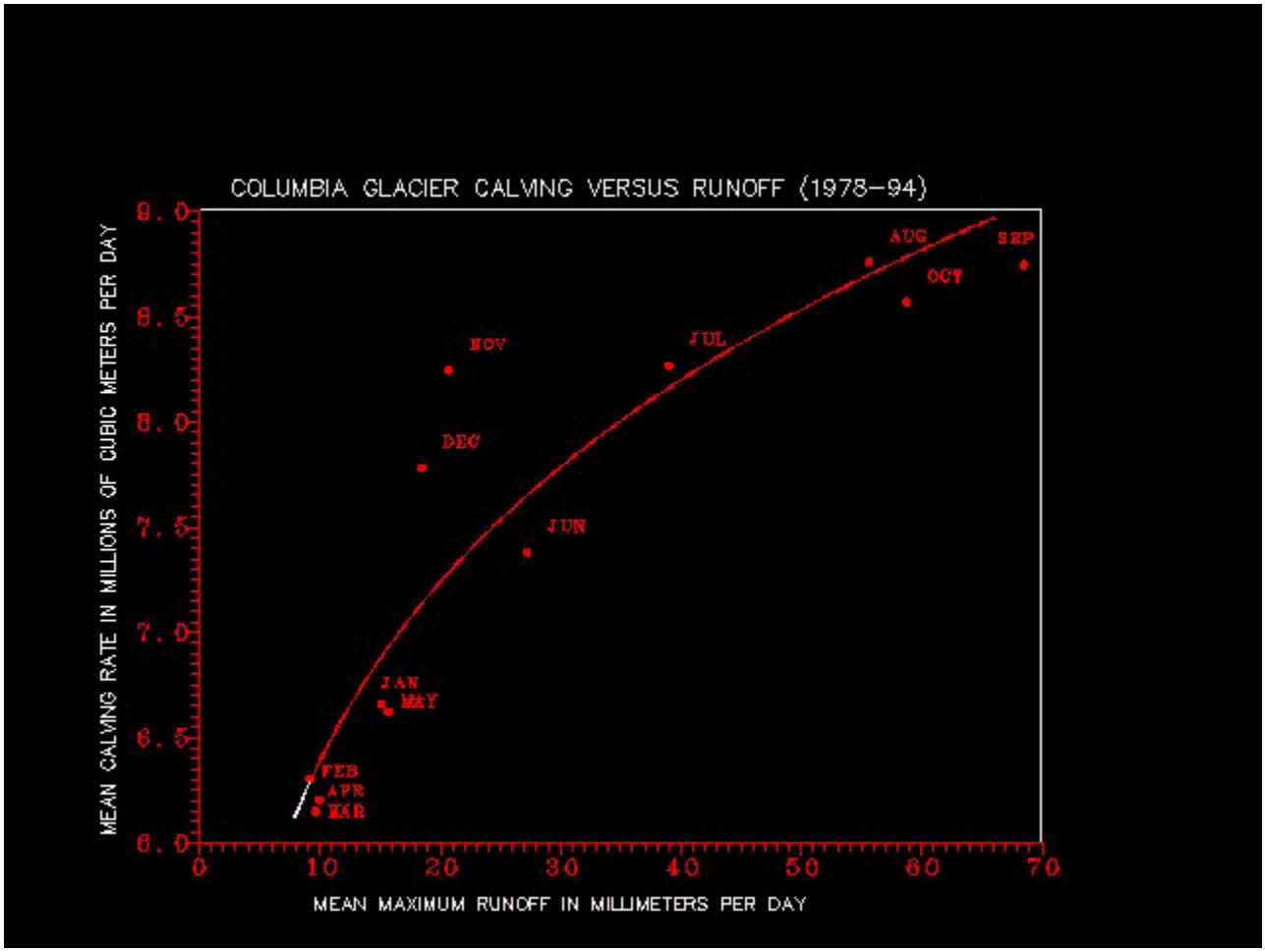

Figure 13. The average monthly calving rate is related to the monthly average of the daily maximum simulated runoff for the 1978-94 period.

For glacier speed versus water storage:

$$G_s = 3.19\ S_{t.0168}$$ (Figure 12),

and for calving rate versus maximum runoff:

$$C_r = 4.23\ R_{x.0179}$$ (Figure 13),

where

G_s = Glacier speed in meters per day,

S_t = Intraglacial storage in mm averaged over glacier area,

C_r = Calving rate in millions of cubic meters per day,

R_x = Maximum simulated runoff in millimeters averaged over glacier area.

The relationships shown in Figures 12 and 13, which are monthly averages calculated over a 10-15 year period, hold up nearly as well on a year-by-year basis. The shape of the curves is nearly the same but there is a positive vertical displacement from year to year. Thus, the fit between these variables is poor when all years are plotted together because another factor directly controls calving rate and indirectly affects glacier speed: water depth at the terminus.

A comparison of simulated runoff and intraglacial water storage with ice motion based on results obtained in the 1987 study suggests that the influx of surface water, not storage, is the most influential in short-term increases of ice speed. Figure 14 shows that a fair agreement exists between flow speed-up events and simulated runoff, but the role of water storage influencing sliding speeds in this case is less clear.

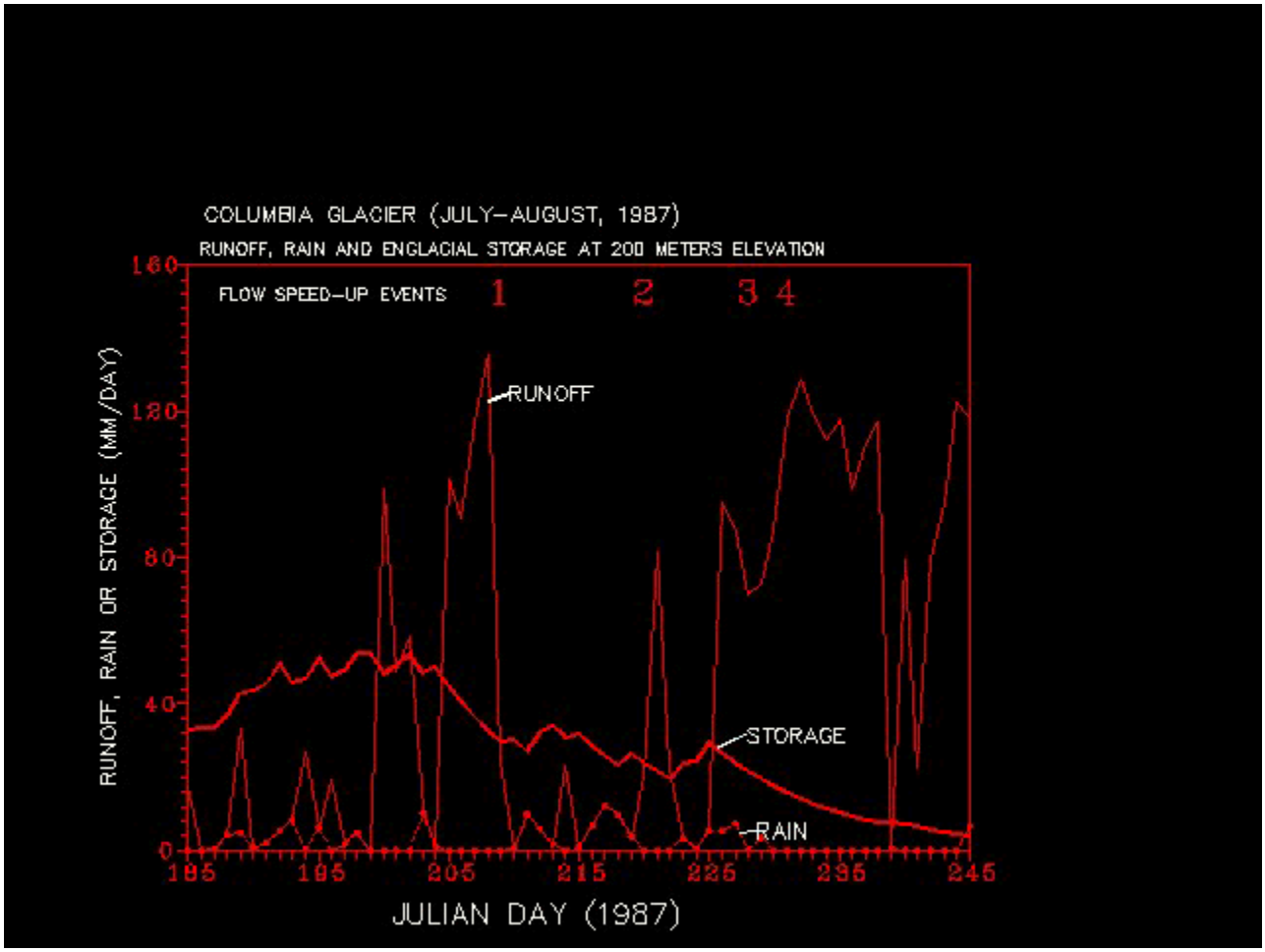

Figure 14. Columbia Glacier runoff at 200 meters elevation is simulated in a mass balance model and is the sum of ablation and precipitation as rain (dashed). Ablation at this elevation at this time of year is primarily ice melt. Intraglacial water storage is derived from daily runoff (see Figure 10). There appears to be a direct connection of the flow speed-up events to simulated runoff, but the relationship to water storage is more complex. Timing of speed-up events is based on velocity measurements made during the 1987 study and taken directly from Figure 4 in Meier and others (1994). Simulated ablation agrees with ablation observations made during this study, but simulated precipitation as rain apparently is too low compared to measured precipitation.

Conclusions

Determining the mass balance of a large glacier that has a high-altitude accumulation area using only low-altitude weather data seems feasible. All of the results given in this study appear physically reasonable, even though the coefficients used to convert weather data to snow accumulation and snow and ice ablation are derived from an unconstrained optimization procedure and could have taken on nearly any value. These results are, of

course, only one set of an infinite number of possible results; however, the PTAA model appears to provide realistic and consistent end-products (over a 17,520 day period and 33-100 meter altitude intervals), of such simulated variables as mass balance, snowline and equilibrium line altitudes, freezing levels, snow accumulation, ablation and runoff. When an end-product (daily runoff) of the mass balance calculation is applied to the problem of finding the reasons for recent changes in ice movement and calving rates of Columbia Glacier, a rational cause and effect relationship is suggested.

Acknowledgments

I am indebted to Bob Krimmel, who supplied all the glacier speed and calving rate data used in this report, to Keith Echelmeyer for the volume change results, and to Dennis Trabant for the area altitude data. I especially would like to thank Austin Post for thirty-five years of being an astute but always fair critic and for not letting me fall into any virtual or real crevasses. I am grateful to Andrea Lewis for editing, word processing and unending moral support. Funding for this study was provided by the author.

References

Brown, C S, M F Meier and A Post (1983), Calving speed of Alaska tidewater glaciers, with application to Columbia Glacier. *U.S. Geol. Surv. Prof. Paper* **1258-C**, 13 pp.

Brozovic, N, D W Burbank and A J Meigs (1997), Climatic limits on landscape development in the Northwestern Himalaya. *Science* **276**, 571-574.

Hooke, R LeB (1984), On the role of mechanical energy in maintaining subglacial water conduits at atmospheric pressure. *Journ. Glaciol.* **30**, 180-187.

Iken, A and R A Bindschadler (1986), Combined measurement of subglacialwater pressure and surface velocity of Findelengletscher, Switzerland: conclusions about drainage system and sliding mechanism. *Journ. Glaciol*. **32**, 101-119.

Kamb, B and five others (1994), Mechanical and hydrologic basis for the rapid motion of a large tidewater glacier, 2. Interpretation. *Journ. Geoph. Res.* **80(B)**, 15,231- 15,244.

Krimmel, R M (1996), Columbia Glacier, Alaska - Research on tidewater glaciers. *U.S. Geol. Surv. Fact Sheet* **FS-091-96**, 4 pp.

LaChapelle, Edward (1962), Assessing glacier mass budgets by reconnaissance aerial photography. *Journ. Glaciol*. **4**, 290-297.

Mayo, L R, and D C Trabant (1978), Surface studies of ice balance and dynamics. In: The Columbia Glacier progress report-December 1977. *U.S. Geol. Surv. Open File Report* **78-264**, 20-34.

Mayo, L R, D C Trabant, R March and W Haeberli (1979), Columbia Glacier stake location, mass balance, glacier surface altitude, and ice radar data-1978 measurement year. *U.S. Geol. Surv. Open File Report* **79-1168**, 79 pp.

Meier, M F and ten others (1978), Columbia Glacier progress report-December l977. *U.S. Geol. Surv. Open-File Report* **78-264**, 56 pp.

Meier, M.F and seven others (1980), Predicted timing of the disintegration of the lower reach of Columbia Glacier, Alaska. *U.S. Geol. Surv. Open File Report* **80-582**, 58 pp.

Meier, M F, and W V Tangborn (1965), Net budget and flow of South Cascade Glacier, Washington. *Journ. Glaciol*. **5**, 547-566.

Nelder, J A and R Mead (1965), A Simplex Method for function minimization. *Computer Journ*. **7**, 308-312.

Pinter, Nicholas and Mark Brandon (1997), How erosion builds mountains. *Scientific American* **276**, 74-79.

Post, A (1975), Preliminary hydrography and historic terminal changes of Columbia Glacier, Alaska. *U.S. Geol. Surv. Hydr. Inv. Atlas* **HA-559**, 3 sheets [supersedes Open File Report 75-491].

Post, A (1977), Reported observations of icebergs from Columbia Glacier in Valdez Arm and Columbia Bay, Alaska, during the summer of 1976. *U.S. Geol. Surv. Open File Report* **77-235**, 3 pp.

Shumskiy, P A (1946), *The energy of glacierization and life of glaciers.* United States Publishing House, Publishing House for Geographical Literature, (Translated by U.S. Snow, Ice and Permafrost Research Establishment, Translation 7, 1950)

Sikonia, W G and A Post (1980), Columbia Glacier, Alaska-Recent ice loss and its relationship to seasonal terminal embayments, thinning, and glacial flow. *U.S. Geol. Surv. Hydr. Inv. Atlas* **HA-619**, 3 sheets. [Supersedes Open File Report 79-1265]

Tangborn, W V (1980), Two models for estimating climate glacier relationships in the North Cascades, Washington, U.S.A. *Journ. Glaciol*. **25**, 3-20.

Tangborn, W V, R M Krimmel and M F Meier (1975), A comparison of glacier mass balance measurements by glaciologic, hydrologic and mapping methods, South Cascade Glacier, Washington. *IAHS Publ*. **104**, 185-196.

Tangborn, W V, A G Fountain and W D Sikonia (1990), Effect of altitude-area distribution on glacier mass balance - A comparison of North and South Klawatti Glaciers, Washington State, U.S.A. *Ann. Glaciol.* **14**, 278-282.

Van der Veen, C J (1995), *Controls on calving rate and basal sliding: observations from Columbia Glacier, Alaska, prior to and during its rapid retreat, 1976-1993*. BPRC Report No. 11, Byrd Polar Research Center, The Ohio State University, Columbus, Ohio, 72 pp.

Van der Veen, C J (1996), Tidewater Calving. *Journ. Glaciol.* **42**,.375-385.

Walters, R (1989), Small-amplitude, short-period variations in the speed of a tide-water glacier in South-Central Alaska, U.S.A. *Ann. Glaciol.* **12**, 187-191.